Chaos, Solitons and Fractals 150 (2021) 111139

Contents lists available at ScienceDirect

Chaos, Solitons and Fractals

Nonlinear Science, and Nonequilibrium and Complex Phenomena

journal homepage: www.elsevier.com/locate/chaos

Fractal structures in the deflection of light by a pair of charged black holes

Edson E. de Souza Filho*, Amanda C. Mathias, Ricardo L. Viana**

Physics Department, Federal University of Paraná, Curitiba, PR, Brazil

ARTICLE INFO

Article history:
Received 4 February 2021
Revised 24 May 2021
Accepted 2 June 2021

Keywords:
Black holes
Fractal structures
Fractal basin

ABSTRACT

The deflection of light by a pair of black holes can be considered an open conservative non-linear dynamic system. The basis of our approach is our understanding of strong gravitational lensing and the geodesic movement of light. We obtain a two-dimensional map that sets out the impact parameter and the escape angle when the light gets deflected by each black hole. Being a non-integrable system, the chaotic area-filling orbits occur in a specific parameter range. Fractal structures are related to the existence of a non-attractive invariant chaotic set. This can be seen in the dynamics of these chaotic orbits. The light-ray that enters the system has two potential defined outcomes. Either the light ray can diverge to infinity or it will fall into one of the two black holes. We describe the escape basins and their boundaries, adopting two methods: firstly the corresponding basin and basin boundary entropies and secondly the computation of the uncertainty exponents.

1. Introduction

Fractal structures are quite common in chaotic systems. Examples are chaotic attractors, basin boundaries, invariant manifolds and others [1]. It is important to note that open chaotic systems present a variety of fractal structures. The so-called strange saddle is caused by the existence of an invariant non-attracting chaotic manifold [2]. Geodesic motions in a curved space are used to describe the dynamics in General Relativity. If the curvature is negative, then there is a sensitive dependence to the initial conditions. This is a necessary condition for chaotic motion, although there are other conditions [3].

The presence of fractal structures in open non-integrable Hamiltonian systems with chaotic motion has been described in many physical manners. Examples include the motion of a star around a galactic center [4,5], open billiards [6,7], drift motion of magnetically confined charged plasma particles [8], magnetic field lines in Tokamaks [9], amongst others.

Cosmic objects such as black holes, produce space-time curvature which leads to the deflection of the light ray as it trace out null geodesics in curved space-time [10]. Systems of binary black holes have been confirmed by the observation of gravitational waves by LIGO Scientific Collaboration [11]. In such systems, where the relative velocities are much lower than the light velocity c, you can consider them as fixed in space.

The null geodesics equations describing the light ray scattering by a pair of black holes are non-integrable and constitute an open conservative dynamical system. This form of chaotic motion is possible [12]. One such example is the Majumdar-Papapetrou binary black hole which occurs when a system of two charged black holes are in static equilibrium due to their electrostatic repulsion [13,14]. Many authors [15,16] have investigated the presence of fractal structures in this system, caused by the chaoticity of geodesic motion [15,16].

The escape basin is a basic fractal structure. It can be investigated in a binary black hole system, which is the array of initial conditions that point to one of three possible outcomes. The light ray can fall in the first black hole; fall into the second black hole or escape to infinity. Escape basins are very important in astrophysical investigations. They are actually the so-called shadows of a black hole. A shadow is a region in the observer's sky which cannot be illuminated by distant light sources due to the blockage of a black hole [17]. Daza and others have studied escape basins in a Majumdar-Papapetrou binary black hole [12,13]. The show that the escape basin boundaries are not just fractal but also display the stronger Wada property: any boundary point belongs to the boundary of at least two other basins.

The investigation of fractal exit basins proposed by de Moura and Letelier produces a two-dimensional map. It describes the scattering of light rays by a system of two static Schwarschild black holes [18]. This is different from the Majumdar-Papapetrou binary

* Corresponding author.
** Principal corresponding author.
E-mail addresses: eesouza@fisica.ufpr.br (E.E. de Souza Filho), viana@fisica.ufpr.br (R.L. Viana).

https://doi.org/10.1016/j.chaos.2021.111139
0960-0779/

black hole system, which requires a numerical integration of the geodesic equations. de Moura's proposal comprises a system where the black holes are supposedly so far apart from each other, that one black hole doesn't affected the other black hole. In this way, the influence of each black hole on the light rays can be studied separately using the exact solution for Schwarschild black holes [18].

In this paper we advance the investigations by considering a system of charged black holes. The charge is important, as charged black holes are said to be the final stage of the collapse of magnetized stars. It is known that black holes in the universe are ruled by the Kerr-Newman metric. We can simplify the system, as the rotation breaks the spherical symmetry and introduces avoidable complications in the calculations. So a general approach enables us to describe each black hole using a spherically symmetrically metric (Reissner-Nordström).

We can use this approximation for the scattering angle by a black hole and combine it with a second black hole to obtain a scattering map similar to that obtained by de Moura and Letelier. However in our case the scattering angle is defined by an analytical method [19]. The second step in our work is to characterize the fractality of the escape basin using the recently developed notion of basin entropy. This is a measure of final state uncertainty related to the fractality of the escape basin boundary [20]. We also use the well-know uncertainty method to obtain the fractal dimension.

This paper is organized as follows: In Section 1 we lay out the basic equations for the scattering of a light ray by a spherically symmetric black hole. In Section 2 we outline the approximate solution of the geodesics equation for the light ray deflection under the gravitational field of two Reissner-Nordström black holes. Section 3 is devoted to the detailing of the two-dimensional scattering map describing the light ray deflection due to the binary black hole system and also discusses some of its dynamical properties. Section 4 contains a description of the corresponding escape basins. Section 5 deals with the characterization of the escape basins using the basin entropy and basin boundary entropy related to them, together with the uncertainty dimension, which is a measure of the fractality of such structures. The last Section contains our Conclusions.

2. Basic equations

In this work, we use the notion of gravitational lensing, which is the deflection of light by a gravitational field. In this case, the lens or gravitational body is a black hole. We define how the light behaves in the vicinity of a black hole using a space-time metric $g_{\mu\nu}$ with signature $(-,+,+,+)$ and constants $c = G = 1$. The light rays follow the geodesic

$$g_{\mu\nu}dx^{\mu}dx^{\nu} = 0, \tag{1}$$

adopting the summation notation and considering a metric for a symmetrically spherical and static space-time with length element,

$$ds^2 = A(r)dt^2 - B(r)dr^2 - C(r)\left(d\theta^2 + \sin^2\theta d\phi^2\right), \tag{2}$$

where $A(r)$, $B(r)$ and $C(r)$ define the metric produced by the black hole.

If a photon approaches the black hole from infinity with impact parameter b, then the substitution of (2) into (1) gives the following general equation for the geodesics

$$\frac{A(r)B(r)}{[C(r)]^2}\left[\frac{d(\phi)}{dr}\right]^2 + \frac{1}{[V(r)]^2} = \frac{1}{b^2}, \tag{3}$$

where $[U(r)]^{-2} = A(r)/C(r)$. After approaching the black hole with a minimum distance r_0 the photon is deflected and emerges out in another direction. From (3) this distance is called the critical impact parameter

$$b_c = \left(\frac{C(r_0)}{A(r_0)}\right)^{1/2} \equiv \left(\frac{C_0}{A_0}\right)^{1/2}. \tag{4}$$

On substituting (4) back into (3) it turns out that the angle of deflection is $\alpha = -\pi + I(r_0)$, where

$$I(r_0) = \int_{r_0}^{\infty} dr\left(\frac{B(r)}{C(r)}\right)^{1/2}\left(\frac{A_0}{A(r)}\frac{C(r)}{C_0}\right)^{-1/2}. \tag{5}$$

In the limit of strong gravitational fields [19], we can expand (5) and use the relation between b and r_0 so as to obtain

$$\alpha(b) = -\bar{a}\ln\left(\frac{b}{b_m} - 1\right) + \bar{c}, \tag{6}$$

where a, $\bar{a}$, c, and $\bar{c}$ depend on the functions A, B, and C, evaluated at the photosphere radius r_m. Similarly to (4) we have $b_m = [C(r_m)/A(r_m)]^{1/2}$.

The evaluation of the coefficients in (6), must be done carefully since the integral (5) diverges at r_0. In order to do so, we rewrite (5) as

$$I(r_0) = \int_0^1 dz f(z, r_0)R(z, r_0), \tag{7}$$

where we define auxiliary variables

$$y = A(r), \qquad y_0 = A_0, \qquad z = \frac{y - y_0}{1 - y_0}, \tag{8}$$

and the following functions

$$N(z, r_0) = \frac{2(ByC_0)^{1/2}}{CA'}(1 - y_0), \tag{9}$$

$$f(z, r_0) = \left\{y_0 - [(1 - y_0)z + y_0]\frac{C_0}{C}\right\}^{-1/2}. \tag{10}$$

Observe that $N(z, r_0)$ is regular for all values of z and r_0, where $f(z, r_0)$ diverges for $z \to 0$. Expanding the integrand of (10) up to second order terms we have

$$f(z, r_0) \approx f_0(z, r_0) = \left(\frac{1}{\gamma z + \beta z^2}\right)^{1/2}, \tag{11}$$

where

$$\gamma = \frac{1 - y_0}{C_0 A'_0}(C'_0 y_0 C_0 A'_0), \tag{12}$$

$$\beta = \frac{(1 - y_0)}{2C_0^2 A'^3_0}\left[2C_0 C'_0 A'^2_0 + (C_0 C'_0 - 2C'^2_0) - C_0 C'_0 y_0 A''_0\right]. \tag{13}$$

Proceeding in this way, we obtain the desired coefficients, namely

$$\bar{a} = \frac{a}{2} = \frac{N(0, r_m)}{2\sqrt{\beta_m}}, \tag{14}$$

$$\bar{c} = c_r + \bar{a}\ln\left(\frac{2\beta_m}{y_m}\right) - \pi, \tag{15}$$

where $\beta_m = \beta(r_m)$ and c_r is the real part of the integral (7).

In this paper, we shall consider Reissner-Nordström black holes, where these functions are given, in a suitable system of units [21], by

$$A(r) = 1 - \frac{2M}{r} + \frac{q^2}{r^2}, \tag{16}$$

$$B(r) = \frac{1}{A(r)}, \tag{17}$$

$$C(r) = r^2. \tag{18}$$

The Reissner-Nordström metric has two event horizons described by the radii where it diverges, at $r_\pm = \frac{3}{4}\{2M \pm [(2M)^2 - \frac{32Q^2}{9}]^{1/2}\}$. Without loss of generality we will rewrite

$$R = \frac{r}{2M}, \qquad Q = \frac{q}{2M}. \tag{19}$$

When $Q \geq 0.5$ there is no event horizon and causality violations appears [22,23], so in this work we are going to use only values of $Q < 0.5$.

For the Reissner-Nordström metric, the coefficients (12) and (13) are given, respectively, by

$$\alpha = \left(2 - \frac{3}{R_0} + \frac{4Q^2}{R_0^2}\right)\frac{R_0 - Q^2}{R_0 - 2Q^2}, \tag{20}$$

$$\beta = \left(\frac{3}{R_0} - 1 - \frac{9Q^2}{R_0^2} + \frac{8Q^4}{R_0}\right)\frac{R_0(R_0 - Q^2)^2}{(R_0^3 - 2Q^2)}. \tag{21}$$

The positive radius of the photosphere (equal to the radius of the event horizon) is

$$R_m = \frac{3}{4}\left[1 + \left(1 - \frac{32Q^2}{9}\right)^{1/2}\right], \tag{22}$$

in such a way that

$$\beta_m = \left[-9 + 32Q^2 - 144Q^4 + 512Q^6 + (9 - 32Q^2)^{1/2} \times (3 + 16Q^2 - 80Q^4)\right]\left[9(Q - 4Q^3)\right]^{-2}. \tag{23}$$

The regular term c_R can't be directly analyzed, however we can expand it in terms of Q, giving

$$c_R = c_{R,0} + c_{R,2}Q^2 + O(Q^4), \tag{24}$$

the first term is

$$c_{R,0} = 2\ln\{6[2 - (3)^{1/2}]\} = 0.9496, \tag{25}$$

and the quadratic correction in Q is

$$c_{R,2} = \frac{8}{9}\left\{(3)^{1/2} - 4 + \ln\left[6\left(2 - (3)^{1/2}\right)\right]\right\} = -1.5939. \tag{26}$$

From these results, it is straightforward to show that the coefficients (14)-(15) of the expansion for the deflection angle (6) are given by

$$\bar{a} = \frac{R_m(R_m - 2Q^2)^{1/2}}{[(2 - R_m)R_m^2 - 2Q^2R_m + 8Q^4]^{1/2}}, \tag{27}$$

$$\bar{c} = -\pi + c_R + \bar{a}\ln\left\{2(R_m - Q^2)^2 \times \frac{[(3 - R_m)R_m^2 - 9Q^2R_m + 8Q^4]}{(R_m - 2Q^2)^3(R_m^2 - R_m + Q^2)}\right\}, \tag{28}$$

$$b_m = \frac{\left[3 + 9(9 - 32Q^2)^{1/2}\right]^2}{4(2)^{1/2}\left[2 - 8Q^2 + (9 - 32Q^2)^{1/2}\right]^{1/2}}. \tag{29}$$

The scattering of a light ray by a single black hole can now be understood in terms of the impact parameter. A light ray comes from infinity and approaches the black hole with impact parameter b and the direction makes an angle ϕ with the reference axis. If $b < b_m$, then the light ray falls into the black hole and disappears. On the other hand, for this light ray not to escape back to infinity, it is necessary that the impact parameter b be such that the scattering angle α is at least π. We thus impose $b > b_{esc}$, where $\alpha(b_{esc}) = \pi$. Using (6) this means that

$$b_{esc} = b_m\left[\exp\left(\frac{\bar{c} - \pi}{\bar{a}}\right) + 1\right]. \tag{30}$$

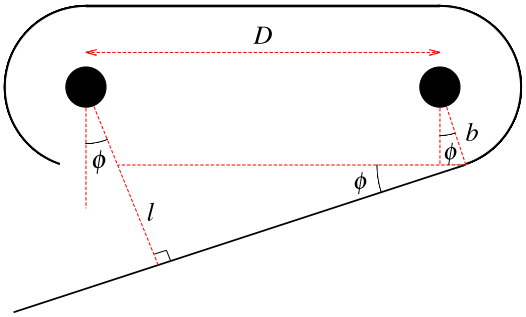

Fig. 1. Scattering map: the trajectory of a light of a light ray on the binary black hole system.

3. The scattering map

In this work, we make use of a system of two identical black holes with equal mass. Binary systems rotate around their center of mass and the LIGO Scientific Collaboration has confirmed the existence of this by the observation of gravitational waves from the merging of two black holes [11]. In such systems, it is possible to consider their relative velocity as fixed in space because it is much smaller than c.

When working with a such a system, there is no exact solution of field equations, unlike the case of a single black hole treated in the previous Section. But the non-linear interaction between their gravitational fields can be neglected if the distance D between the black holes is bigger than their Schwarzschild radius $2M$.

In this case, we consider the deflection of light from each black hole in a separate way using the expressions previously found for the Reissner-Nordström metric. In other words, the scattering of light by a given black hole ignores the effect of the other black hole. Similar approximations for the Schwarzschild metric are discussed in detail in Ref. [18]. In particular, they may not hold if we consider the scattering of massive test particles.

The axial symmetry axis is the line connecting the two black holes. Assume that the light rays have zero angular momentum in this direction. The light rays are constrained to move in the plane containing the two black holes. Fig. 1 shows the basic geometry involved in the light scattering by the system. Coming from infinity, a light ray approaches the first black hole with impact parameter b in a direction that makes an angle ϕ with the axial symmetry axis. So for this light ray not to escape back to infinity, it is necessary that $b > b_{esc}$, where b_{esc} is given by (30).

We don't want the light ray to fall in the first black hole as soon as they meet, so the impact parameter must be $b < b_m$. If the light ray is not deflected to infinity by the first black hole, it goes to the other black hole and is again deflected. If not deflected to infinity, it returns to the vicinity of the first black hole, and so on.

For convenience we define discrete variables (b_n, ϕ_n) to be the impact parameter and escape angle respectively. With reference to the symmetry axis in the neighborhood of the nth scattering. Odd (Even) values of n correspond to the second (first) black hole. Using such definitions the differential equations for light scattering reduce to a discrete map.

$$b_{n+1} = b_n + D\phi_n, \tag{31}$$

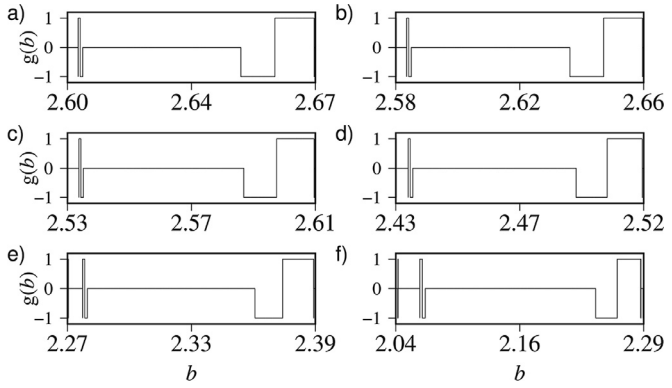

Fig. 2. For $\phi = 0$, we variate the charge from 0 to 0.49 and we plot the corresponding values of the function $g(b)$ (see text for details). *a*) for 0, *b*) for 0.1, *c*) for 0.2, *d*) for 0.3, *e*) for 0.4 and *f*) for 0.49.

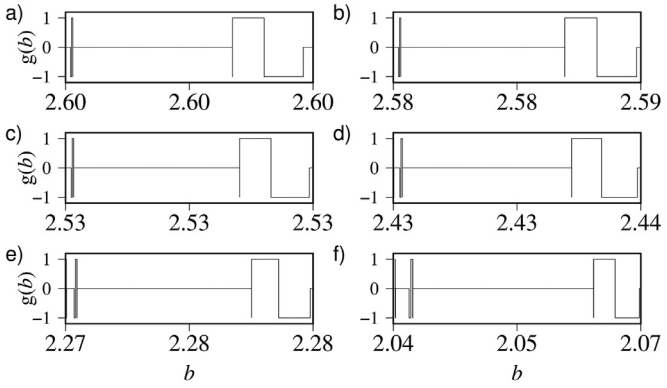

Fig. 3. First approximation for $\phi_0 = 0$ which correspond to the charge value of *a*) for 0, *b*) for 0.1, *c*) for 0.2, *d*) for 0.3, *e*) for 0.4 and *f*) for 0.49.

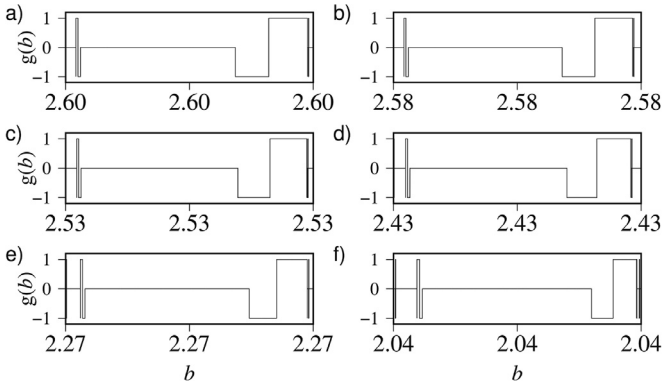

Fig. 4. Second approximation for $\phi_0 = 0$ which correspond to the charge value of *a*) for 0, *b*) for 0.1, *c*) for 0.2, *d*) for 0.3, *e*) for 0.4 and *f*) for 0.49.

$$\phi_{n+1} = \pi + \phi_n - \alpha(b_{n+1}), \mod 2\pi \tag{32}$$

called the scattering map [18]. Some sign conventions are essential: positive values of b imply that the light ray goes from black hole 1 to 2 (from "right" to "left" in Fig. 1), and negative values signify the opposite; whereas positive values of ϕ correspond to counterclockwise rotations.

4. Escape basins

Our system of black holes fits the model of open dynamical systems whereby trajectories in that system will eventually escape from the phase space region. As there are different ways that the light ray can escape from the two black holes system, we can analyze the initial conditions that make the particles escape through a given exit. This set of initial conditions is called the escape basins. When we have two or more exits, we can point out the boundary that divides the basins [24]. It is long known that conservative dynamical systems with chaotic dynamics have fractal escape basins and fractal escape basin boundaries [1].

To obtain the escape basins we use the scattering map (31)-(32). We isolate the phase space region $\iota = \{0 \leq \phi_0 \leq 2\pi, b_m < b_0 < b_{esc}\}$ in a extensive number of points (a set of initial conditions (b_0, ϕ_0)). We iterate the map and observe which exit they escape to, saving the outcome for each point.

After a number of map iterations, the light ray may fall into one black hole (**A**), into the other black hole (**B**), or escapes in the direction of infinity (**C**). This depends on the initial conditions. All outcomes can be treated as exits. We stop iterating the map once a light ray goes into one of the exits. Accordingly, we denote the corresponding escape basins to be $\mathcal{B}(\mathbf{A})$, $\mathcal{B}(\mathbf{B})$ and $\mathcal{B}(\mathbf{C})$.

Labeling the black holes **A** and **B** is immaterial, because their escape basins would be symmetric, i.e. they have the same size. As well it is expected that the dominant basin will be the infinity one (**C**). Following the analyses requires further magnifications as sequences of exits cant be observed. In order to better understand the exits, we define a function $g(b)$ such that $g(b) = 1$. If the orbit falls into black hole **A**, $g(b) = -1$, if it falls into **B**, and $g(b) = 0$ if the orbit escapes to infinity [18].

As we are working with the Reissner-Nordström metric, we want to see how the basin will behave when we have different charge values. As we defined previously, the charge has a limit of $Q \leq 0.5$. Analyzing two regions, defined as $\phi_0 = 0$ and $\phi_0 = \pi$. For the impact parameter we divided $b_m < b < b_{esc}$ in to 10^6 points. For $\phi_0 = 0$ we vary the value of Q from 0 to 0.49. Iterating the map for each value, we plot the escape basin in Fig. 2 a) to f), the pattern maintains the same visual appearance for each charge, but the range of b changes. To assess if the basins are fractals, we make an approximation in the zone where there is a rapid variation of escape direction. So Fig. 3 shows us the respective first approximation. The pattern repeats itself from Fig. 2 with little difference. We take another approximation in Fig. 3 to obtain Fig. 4. Again the pattern is the same as Figs. 2 and 3. For $\phi_0 = \pi$ the results are similar.

That shows us that the system is fractal. For this analysis of the escape basins the metric of Reissner-Nordström is visually indistinguishable to the Schwarzschild. The difference comes from the fact that the particle passes closer to the black hole as the charge increases (b range goes from 2.6 to 2.04).

This can be explained looking at the impact parameter definition as detailed in [25]. It shows that in the study of gravitational lensing $b = D_{ol}\theta$ where θ is the position of the formed image. D_{ol} is the distance between the observer and the lens. We use a black hole as gravitational lens as a base for our study. If the image position results decrease as the charge is increased then the impact parameter results will behave similarly.

5. Dimension and entropy

Given the complex nature of this boundary, we analyze the fractality of the system using two quantitative characterizations of the escape basin boundary. First we determinate the basin entropy and basin boundary entropy. Next we compute the uncertainty exponent of the escape basin boundary by using the uncertainty fraction method.

In this work, we use the proposed method of basin entropies, which quantifies the degree of uncertainty due to the fractality

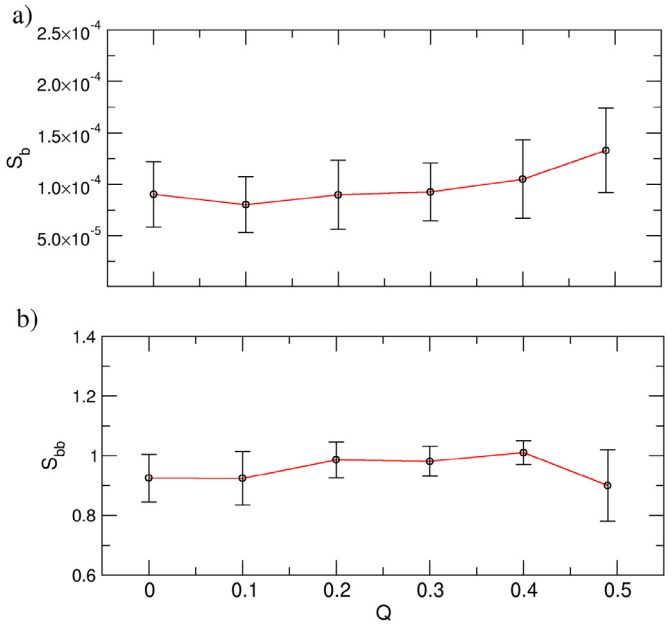

Fig. 5. The basin entropy S_b and the basin boundary entropy S_{bb} for each charge Q when $\phi_0 = 0$.

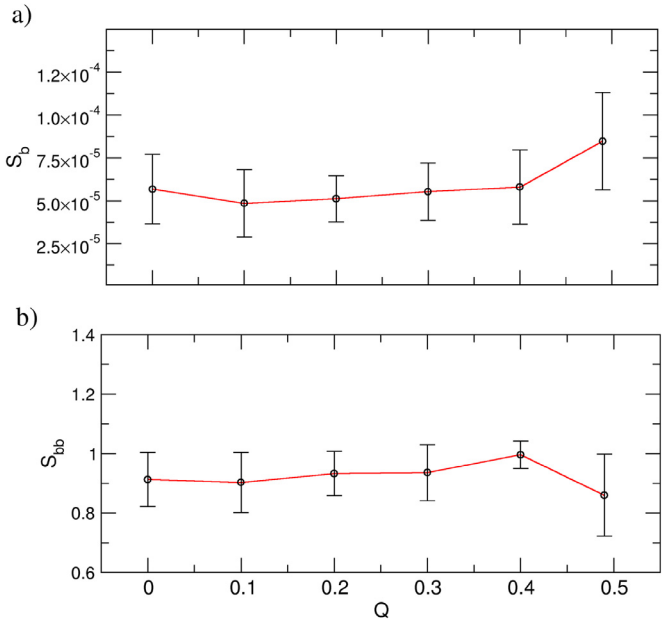

Fig. 6. The basin entropy S_b and the basin boundary entropy S_{bb} for each charge Q when $\phi_0 = \pi$.

of basin. The basic idea of this method is as follows: for a single basin or unique exit, the corresponding probability is equal to unity ($p_A = 1$), hence the basin entropy is zero ($S_b = 0$). This means zero uncertainty, whereas for N_A equiprobable basins or exits, the corresponding probability is $p_A = N_A$, thus the basin entropy is $S_b = \ln N_A$. This gives a completely randomized basin structure.

The basin boundary entropy S_{bb}, quantifies the complexity of the basin boundary. There are also limit situations that separate basins with smooth boundaries from those with fractal boundaries. Suppose that the basins were separated by a smooth boundary, then the maximum value possible is $S_{bb} = \ln 2$. This would be a case of only two basins, where every box computed in the boundary contains equal proportions. If $S_{bb} > \ln 2$, the basin boundary is fractal. This is a sufficient but not a necessary criterion for fractality, i.e., there are fractal boundaries even if $S_{bb} < \ln 2$.

We computed the basin entropies of $\phi_0 = 0$ and $\phi_0 = \pi$. We considered boxes with 4, 5, 8 and 10 initial conditions per box and then we iterated each initial condition for a maximum number of 10^4 iterations of the map. We excluded from the statistics those initial conditions leading to orbits that do not escape. For $\phi_0 = 0$ and $\phi_0 = \pi$, we computed the probabilities of points into each box corresponding to the exits A, B and C. Thus, the entropy entropy for each box is

$$S = -p_A \log p_A - p_B \log p_B - p_C \log p_C. \tag{33}$$

Then, the total basin entropy is the summation of the basin entropy of each box divided by the total number of boxes N: $S_b = S/N$ and the basin boundary entropy is $S_{bb} = S/N_b$, where N_b is the number of boxes that containing points of the boundary.

Fig. 5 show the results. For each value of charge Q for $\phi_0 = 0$ then (a) shows the basin entropy and (b) the basin boundary entropy of the escape basin. Fig. 6 show the results of S_b in (a) and S_{bb} in (b) corresponding to the case $\phi = \pi$. The results suggests that the basin entropy and the basin boundary entropy take on the same values for each value of charge Q, within the uncertainty of our measurements.

The corresponding values are $S_b(\phi_0 = 0) = 9.846 \times 10^{-5} \pm 3.330 \times 10^{-5}$ and $S_b(\phi_0 = \pi) = 5.90 \times 10^{-5} \pm 2.00 \times 10{-}5$ for the

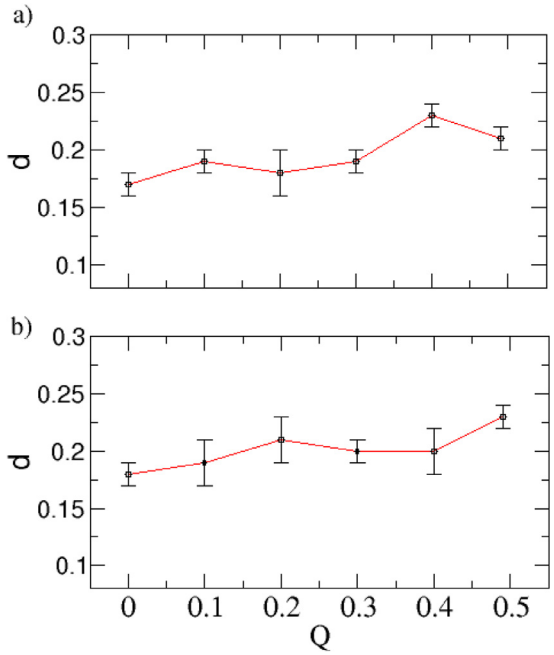

Fig. 7. Dimensions of each basin as the charge Q changes for *a)* $\phi_0 = 0$ and *b)* $\phi_0 = \pi$.

basin entropy. $S_{bb}(\phi_0 = 0) = 0.954 \pm 0.070$ and $S_{bb}(\phi_0 = \pi) = 0.923 \pm 0.090$ for the basin boundary entropy. For $\phi_0 = 0$ and $\phi_0 = \pi$ the value of S_b is low, and accordingly, $S_{bb} > S_b$, since the number of boxes containing the boundary is generally less than the total number of boxes. However, $S_{bb} > \ln 2$, i.e. the basin boundary is fractal for two cases.

As a general trend, the degree of complexity of the basin increases with the charge of the black holes Q. We can observe in Fig. 5b) that the basin boundary entropy increases as the charge goes from 0 to 0.4 and suffers a decrease afterwards for $Q = 0.49$. The same happens in Fig. 6b). The increase of basin entropies

means that their structures become progressively more mixed as the charge of the black holes increases.

To go further and confirm the fractality of the system we computed the uncertainty dimension of the escape basin boundary by using the uncertainty fraction method. The uncertainty dimension d quantifies the final-state uncertainty of the points belonging to basin boundary. Thus, we obtained the fraction of uncertain initial conditions $f(\epsilon)$ varying the uncertainty (ϵ) for the two cases of ϕ_0 varying the charge Q. After this, we obtain the uncertainty exponent (α). Since $\alpha = K - d$, where $K = 1$, in our case, a smooth boundary with $d = 0$, has $\alpha = 1$, whereas $0 < \alpha < 1$ characterizes a fractal boundary.

We computed the uncertainty dimension of the escape basin boundary for $\phi_0 = 0$ and $\phi_0 = \pi$, the results being shown in Fig. 7a) and b), respectively. The variable parameter is the charge Q. The maximum dimension value for $\phi_0 = 0$ occurs in $Q = 0.4$ and has $d = 0.218 \pm 0.005$. The corresponding maximum dimension value for $\phi_0 = \pi$ occurs in $Q = 0.49$ and has $d = 0.244 \pm 0.012$. This therefore suggests that the escape basin boundaries are fractals and consistent with the results obtained for the basin entropies.

6. Conclusion

A system of two black holes yields important information about how the behavior of the universe. Investigating gravitational waves is key to unlocking this information and so analysis of binary systems is crucial. We studied how light behaves when enters a system of two black holes. The distance between the black holes is such, that the system is simplified and we can analyze the behave in each black hole separably. Reissner-Nordström black holes are static and have the charge as one of their characteristics making it closer to a real black hole. In this work, we varied the charge from 0 (Schwarzschild) to 0.49 which is the limit for a Reissner-Nordström black hole with event horizon.

The black holes behave as a system but work individually. Strong gravitational lensing allows us to describe the light movement by a two-dimension map. We chose two fixed points for the escape angle. We ran the map giving the initial conditions for the parameter of impact. The light ray can escape in three directions; into the first black hole, into the second black hole or escaping to infinity.

We plotted the escape for each initial condition and analyzed the patterns exhibited. We observed zones where the region of escape varies rapidly and where chaos exists. We did an approximation exactly at the chaos zones and saw that the pattern repeats itself. Another approximation gives the same results. This indicates that the system is fractal.

It is important to highlight that all the plots have the same structure as the Schwarzschild case, but with a different range of the impact parameter. This is explained by the lensing study that shows that the position of the images produced by Reissner-Nordström black holes are closer to each other than the Schwarzschild. As the charge increases, they get closer and closer. The impact parameter is proportional to the image position and so we can see that as the charge increases then the impact parameter decreases.

We considered two approaches to confirm the fractal characteristic of the system. Firstly, we considered the entropy method where if the value of the basin boundary is greater than $\ln 2$, then the system is fractal, giving us a parameter of comparison. For every case proposed, our results show that the basin boundary is greater than $\ln 2$. Secondly, we considered the dimension where $d = 0$ is smooth and $d = 1$ total fractal. Our results again confirm that the system is fractal and that the small value of d results from having a very smooth area where the light ray escapes to infinity.

In this paper, we analyzed the binary Reissner-Nordström black hole system. If we iterate a two-dimension map, varying the charge values, then we discovered that the system has fractal characteristics and that there is no major difference structurally from Reissner-Nordström to Schwarzschild when within the given parameters for a black hole with event horizon to exist.

Declaration of Competing Interest

The authors declare that they have no known competing financial interests or personal relationships that could have appeared to influence the work reported in this paper.

CRediT authorship contribution statement

Edson E. de Souza Filho: Conceptualization, Data curation, Formal analysis, Investigation, Methodology, Resources, Software, Supervision, Validation, Visualization, Writing - original draft. **Amanda C. Mathias:** Data curation, Formal analysis, Investigation, Validation, Visualization, Writing - original draft. **Ricardo L. Viana:** Conceptualization, Funding acquisition, Methodology, Project administration, Resources, Supervision, Validation, Visualization.

Acknowlgedgments

The author acknowledges the valuable help of Adriane da S. Reis, Eduardo L. Brugnago and Davis McComb. This document is the result of the research project funded by the Coordenação de Aperfeiçoamento de Pessoal de Nível Superior-CAPES [(Proc. 88882.344169/2015-01), (Proc. 88887.320059/2019-00)], Conselho Nascional de Desensolvimento Científico e Tecnológico - CNPq (Proc. 301019/2019-3).

References

[1] Aguirre J, Viana RL, Sanjuán MAF. Fractal structures in nonlinear dynamics. Rev Mod Phys 2009;81:333–86. doi:10.1103/RevModPhys.81.333.
[2] Péntek A, Toroczkai Z, Tél T, Grebogi C, Yorke JA. Fractal boundaries in open hydrodynamical flows: Signatures of chaotic saddles. Phys Rev E 1995;51:4076–88. doi:10.1103/PhysRevE.51.4076.
[3] Dettmann CP, Frankel NE, Cornish NJ. Fractal basins and chaotic trajectories in multi-black-hole spacetimes. Phys Rev D 1994;50:R618–21. doi:10.1103/PhysRevD.50.R618.
[4] Aguirre J, Vallejo JC, Sanjuán MAF. Wada basins and chaotic invariant sets in the Hénon-Heiles system. Phys Rev E 2001;64:066208. doi:10.1103/PhysRevE.64.066208.
[5] Barrio R, Blesa F, Serrano S. Fractal structures in the Hénon-Heiles hamiltonian. EPL 2008;82(1):10003. doi:10.1209/0295-5075/82/10003.
[6] Altmann EG, Leitão JC, Lopes JV. Effect of noise in open chaotic billiards. Chaos 2012;22(2):026114. doi:10.1063/1.3697408.
[7] Hansen M, da Costa DR, Caldas IL, Leonel ED. Statistical properties for an open oval billiard: an investigation of the escaping basins. Chaos Solitons Fractals 2018;106:355–62. doi:10.1016/j.chaos.2017.11.036.
[8] Mathias AC, Viana RL, Kroetz T, Caldas IL. Fractal structures in the chaotic motion of charged particles in a magnetized plasma under the influence of drift waves. Physica A 2017;469(C):681–94. doi:10.1016/j.physa.2016.11.049.
[9] Mathias A, Kroetz T, Caldas I, Viana R. Chaotic magnetic field lines and fractal structures in a tokamak with magnetic limiter. Chaos Solitons Fractals 2017;104:588–98. doi:10.1016/j.chaos.2017.09.017.
[10] Misner CW, Thorne KS, Wheeler JA. Gravitation. WH Freeman and Co San Francisco; 1973. ISBN 0716703440,978-0716703440
[11] Abbott BP, Abbott R, Abbott TD, et al. Observation of gravitational waves from a binary black hole merger. Phys Rev Lett 2016;116:061102. doi:10.1103/PhysRevLett.116.061102. LIGO Scientific Collaboration and Virgo Collaboration
[12] Daza A, Shipley JO, Dolan SR, Sanjuán MAF. Wada structures in a binary black hole system. Phys Rev D 2018;98:084050. doi:10.1103/PhysRevD.98.084050.
[13] Majumdar SD. A class of exact solutions of Einstein's field equations. Phys Rev 1947;72:390–8. doi:10.1103/PhysRev.72.390.
[14] Papapetrou A. A static solution of the equations of the gravitational field for an arbitrary charge-distribution. Proc R Irish Acad Sect A 1945;51:191–204.
[15] Contopoulos G. Asymptotic curves and escapes in hamiltonian systems. Astron Astrophys 1990;231(1):41–55.
[16] Contopoulos G, Kandrup HE, Kaufmann D. Fractal properties of escape from a two-dimensional potential. Physica D 1993;64(1):310–23. doi:10.1016/0167-2789(93)90262-Y.

[17] Cunha PVP, Herdeiro CAR. Shadows and strong gravitational lensing: a brief review. Gen Relativ Gravitation 2018;50(4):42. doi:10.1007/s10714-018-2361-9.
[18] de Moura APS, Letelier PS. Scattering map for two black holes. Phys Rev E 2000;62:4784–91. doi:10.1103/PhysRevE.62.4784.
[19] Bozza V. Gravitational lensing in the strong field limit. Phys Rev D 2002;66:103001. doi:10.1103/PhysRevD.66.103001.
[20] Daza A, Wagemakers A, Georgeot B, Guéry-Odelin D, Sanjuán MAF. Basin entropy: a new tool to analyze uncertainty in dynamical systems. Sci Rep 2016;6(1):31416. doi:10.1038/srep31416.
[21] Chandrasekhar S. The mathematical theory of black holes. OUP Oxford, Oxford; 1998.
[22] Carter B. Global structure of the kerr family of gravitational fields. Phys Rev 1968;174:1559–71. doi:10.1103/PhysRev.174.1559.
[23] Hawnking S, Ellis GFR. The large scale structure of space-time. Cambridge University Press, Cambridge; 1973.
[24] Bleher S, Grebogi C, Ott E, Brown R. Fractal boundaries for exit in hamiltonian dynamics. Phys Rev A 1988;38:930–8. doi:10.1103/PhysRevA.38.930.
[25] Eiroa EF, Romero GE, Torres DF. Reissner-Nordström black hole lensing. Phys Rev D 2002;66:024010. doi:10.1103/PhysRevD.66.024010.